Roll Force, Torque, Lever Arm Coefficient, and Strain Distribution in Edge Rolling

S.-E. Lundberg and T. Gustafsson

Due to the growing importance of width control in strip and plate mills, edge rolling is currently an important process in hot rolling mills. Research in edge rolling has been carried out, and in the present article, models for roll force, torque, and lever arm coefficient are derived using the upper bound method. A simple, kinematically admissible deformation zone and velocity field, independent of friction in the roll gap, is proposed, and the energy dissipation rate is derived. The formula for energy dissipation rate has, in practice, no limitation because all edge rolling geometries are safely in the area where the formula is valid. Roll force and torque are derived by means of two independent integrals. Thus, the lever arm coefficient is evaluated from the expressions for roll force and torque using conventional rolling theory. Rolling trials report good agreement with theory. Measured roll forces are similar to calculated forces. Furthermore, the shape of the dogbone that arises during edge rolling is in fairly good agreement with the calculated dogbone shape. Deviations are due to the deviation from ideally plastic material in the experiments. Also, the strain distribution over the dogbone is similar to the proposed deformation zone. Thus, a new formula has been developed to a stage that it can be implemented in width control systems for edge rolling stands in hot strip and plate mills.

Keywords

edge rolling, lever arm coefficient, roll force, roll torque, strain distribution, upper bound analysis

1. Introduction

IN recent years, control of slab width during rolling has become increasingly important.[1-6] The reason for improved width control is the increased amount of continuous casting and the adaptation of hot material flow in the entire mill. To reduce downtime in the continuous casting plant, the goal is to reduce the number of slab sizes. Thus, the necessity to change slab width during rolling increases. For smaller changes in width, the natural spread during rolling can be used.[7] If greater changes in slab width are necessary, Hi-spread technology must be used.[8] Spreading of slabs is unfortunately not enough to achieve the necessary flexibility in rolling of strip and plate, and edge rolling is the other important measure to control the width of the rolled product.[1,6] With increasing demand on the mills, research in the area of edge rolling has been initiated.[9] Different methods have been used to describe the deformation of material during edge rolling,[9-13] and in previous work, a model for roll torque calculation was derived.[14] In the current work, a complete analysis of edge rolling was carried out, using the upper bound method for analysis.

2. Roll Force, Torque, and Lever Arm Coefficient in Edge Rolling

2.1 *Background—Upper Bound Solution*

From the basic knowledge that edge rolling always results in dogbone formation of the rolled slab, a simple kinematically admissible deformation zone and velocity field, independent of friction in the roll gap, was designed, according to Fig. 1, for derivation of roll torque. From the derivation,[14] the energy dissipation rate was found to be equal to:

$$\dot{W} = 2k \cdot R^2 \cdot \omega \left[(1 - \cos\alpha)(h_o - \tfrac{1}{2}R\cos\alpha) + \tfrac{1}{8}R(1 - \cos 2\alpha) \right] \quad [1]$$

List of Symbols

A, A', B, B', C, C', D	Points in deformation zone in upper bound solution
F	Roll force
R	Roll radius
T	Roll torque
$\dot{W}$	Energy dissipation rate
X	Lever arm
a	Lever arm coefficient
b	Full width of rolled slab
dt	Increment of time
dw	Slab width derivative
$\overline{dw}$	Mean slab width derivative in roll gap
$d\varphi$	Increment of rolling angle
h_o	Entry thickness of rolled slab
k	Shear yield stress
p	Roll pressure
v	Roll velocity
w	Half width of rolled slab
w_o	Half entry width of rolled slab
w_1	Half exit width of rolled slab
α	Bite angle
β, γ	Arbitrary angles
φ	Arbitrary angle in roll gap
φ_n	Neutral angle
ψ	Dimensionless value of energy dissipation rate
ω	Angular velocity of roll

S.-E. Lundberg and **T. Gustafsson,** Milltek Innovation, Box 351, S-801 05 Gävle, Sweden.

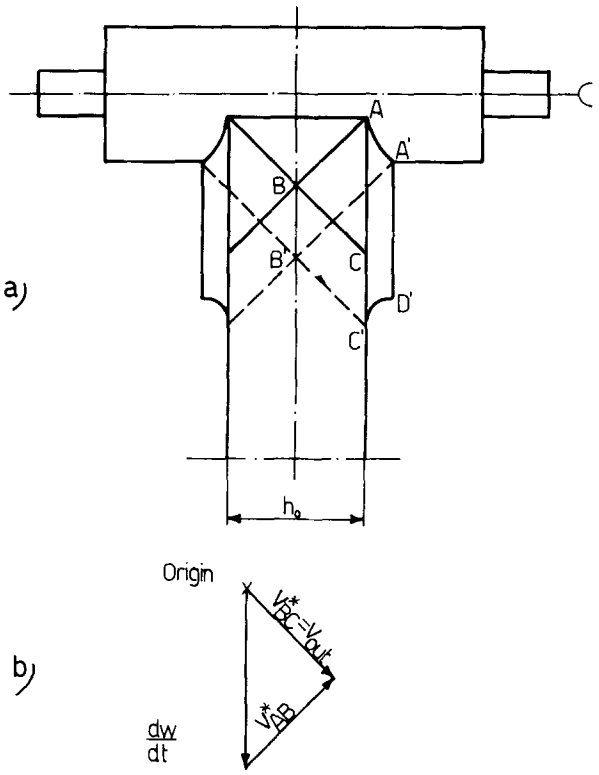

Fig. 1 Proposed upper bound solution. (a) Deformation zone. (b) Hodograph.

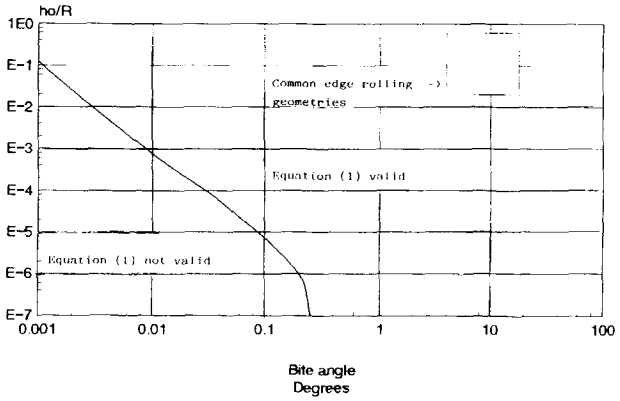

Fig. 2 Limitations of Eq 1.

During analysis of the reliability of Eq 1, it was rearranged to:

$$\psi = \frac{\dot{W}}{2k \cdot \omega \cdot R^3} = (1 - \cos\alpha)\left(\frac{h_o}{R} - \frac{1}{2}\cos\alpha\right) + \frac{1 - \cos 2\alpha}{8} \quad [2]$$

It is now obvious that the equation in reality consists of two terms of the same order of magnitude. The second factor of the first term can be a positive or a negative number, depending on the values of h_o/R and α. If $\frac{1}{2} \cos \alpha > h_o/R$, the whole first term of Eq 2 will be negative, and the second term must always be a higher positive number, unless energy would be produced in the process, i.e., the edge rolling process would be a perpetuum mobile. This is the limitation of Eq 2 and thus of Eq 1. To evaluate the limit of validity of the model, Eq 2 was solved for combinations of h_o/R and α by means of a special computer program using incremental steps of 10^{-3} for both factors. The results from these calculations are shown in Fig. 2. In this figure, common edge rolling geometries are illustrated, and it is apparent that there is no geometric limit to the formula.

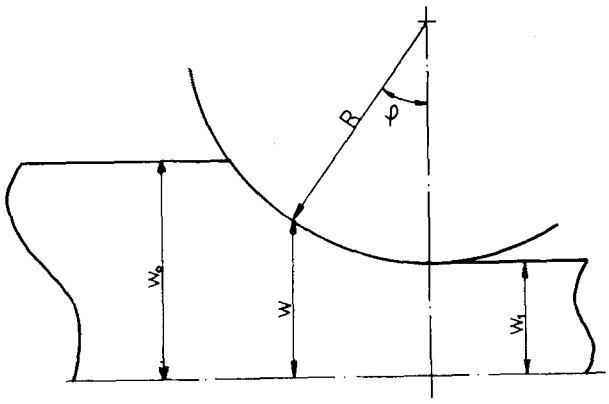

Fig. 3 Definition of angle φ.

2.2 *Roll Force*

The energy dissipation rate can be written as:

$$\dot{W} = F\frac{dw}{dt} \quad [3]$$

The change in width, dw/dt, can be derived from Fig. 3, where the half width of the slab is

$$w = w_1 + R(1 - \cos\varphi) \quad [4]$$

and

$$\frac{dw}{d\varphi} = R \cdot \sin\varphi \quad [5]$$

Using

$$\frac{d\varphi}{dt} = \omega \quad [6]$$

and

$$v = \omega \cdot R \quad [7]$$

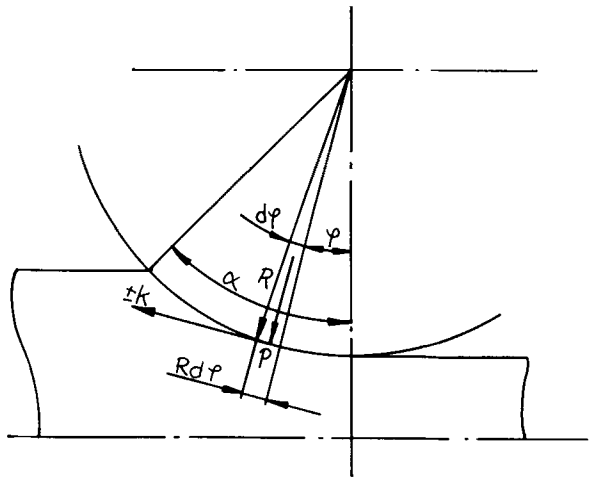

Fig. 4 Tangential force in the roll/bar interface.

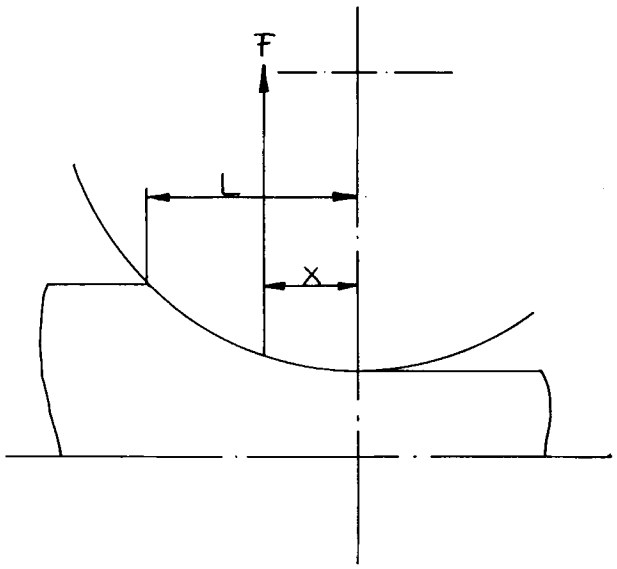

Fig. 5 Simplified assumption for roll torque calculation.

yields

$$\frac{dw}{dt} = \omega \cdot R \cdot \sin \varphi \qquad [8]$$

Substituting Eq 8 into Eq 3, the energy dissipation rate is equal to

$$\dot{W} = F \cdot \omega \cdot R \cdot \sin \varphi \qquad [9]$$

Because the value of sin φ is not constant over the arc of contact, the roll force is found by substituting *dw/dt* in Eq 9 by the mean value and found by integrating Eq 8 over the arc of contact

$$\frac{\overline{dw}}{dt} = \frac{1}{\alpha}\int_0^{\alpha} \omega \cdot R \cdot \sin d\varphi \qquad [10]$$

i.e.,

$$\dot{W} = \frac{F \cdot \omega \cdot R(1 - \cos \alpha)}{\alpha} \qquad [11]$$

By equalizing Eq 11 to Eq 1, the roll force is written as:

$$F = 2k \cdot R \cdot \alpha \left\{ h_o + \frac{R}{2}\left[\frac{1 - \cos 2\alpha}{4(1 - \cos \alpha)} - \cos \alpha \right] \right\} \qquad [12]$$

2.3 *Roll Torque and Lever Arm Coefficient*

The basic theory of roll torque is discussed, among others by Klarin, Mouton, and Lundberg.[15] The tangential force acting on a length $Rd\varphi$ of the arc of contact of one roll is $kRd\varphi$, assuming sticking friction in the entire contact zone. The torque about the roll axis, exerted by this force, is $kR^2d\varphi$ (see Fig. 4). The total torque acting on the roll is obtained by integrating over the arc of contact, with due regard to the direction in which *k* acts. On the entry side of the roll gap, the material moves slower than the roll, and the friction counteracts the movement of the roll. On the exit side of the roll gap, however, the material moves faster than the roll, and the frictional force acts in the same direction as the roll rotation. Now, if a positive torque is that which must be overcome by the mill drive motor, the torque arising from the entry side is positive and that on the exit side is negative. Then, for two rolls, the total torque, *T*, is

$$T = 2 \cdot R^2 \cdot b \cdot k \cdot \left(\int_{\varphi_n}^{\alpha} d\varphi - \int_0^{\varphi_n} d\varphi \right)$$
$$= 2 \cdot R^2 \cdot b \cdot k \cdot (\alpha - 2\varphi_n) \qquad [13]$$

Generally, the neutral angle (φ_n) is somewhere near the middle of the arc of contact[16] and ($\alpha - 2\varphi_n$) is a small quantity. Equation 13 therefore leads to inaccuracy, because the neutral angle is only approximately known, and a small error in the neutral angle leads to a significant error in roll torque.

An alternate expression for roll torque is obtained by considering the equilibrium of horizontal forces in the roll gap. This gives an equation for roll torque, independent of φ_n, as:

$$T = 2 \cdot R^2 \cdot b \cdot \int_0^{\alpha} p\varphi d\varphi \qquad [14]$$

Very often in engineering calculations, the roll torque is determined by assuming that the resulting roll force is acting on a distance *X* from the exit plane (Fig. 5). The roll torque (on two rolls) is then:

$$T = 2 \cdot F \cdot X \quad [15]$$

Expressing X as a fraction of the arc of contact, the roll torque can be written as:

$$T = 2 \cdot F \cdot a \cdot L \quad [16]$$

where L is equal to

$$L = R \cdot \sin \alpha \quad [17]$$

The lever arm coefficient, a, is not a physically determined quantity, but a calculation coefficient used for a simplified roll torque calculation procedure, as discussed in detail by Kastner and Kastner.[17]

In a previous paper,[14] an expression for roll torque on two rolls was derived:

$$T = 2 \cdot 2k \cdot R^2 \cdot [(1 - \cos \alpha)(h_o - \tfrac{1}{2}R \cos \alpha) + \tfrac{1}{8}R(1 - \cos 2\alpha)] \quad [18]$$

Because the roll force and torque are determined by means of two independent integrals derived from the same velocity field, the lever arm coefficient can be found by the same procedure that was applied to the slip-line field analysis of rolling.[15] Rearranging Eq 16 yields:

$$a = \frac{T}{2 \cdot F \cdot R \cdot \sin \alpha} \quad [19]$$

The expressions for T and F (Eq 18 and 12) are inserted in Eq 19, and a is evaluated to:

$$a = (1 - \cos \alpha)/\alpha \cdot \sin \alpha \quad [20]$$

Using

$$(1 - \cos \beta)/2 = \sin^2(\beta/2) \quad [21]$$

and

$$\sin(\beta + \gamma) = \sin \beta \cdot \cos \gamma + \sin \gamma \cdot \cos \beta \quad [22]$$

Putting

$$\beta = \gamma = \alpha/2 \quad [23]$$

Eq 20 can be written as:

$$a = \frac{1}{\alpha} \cdot \frac{2 \cdot \sin^2(\alpha/2)}{2 \cdot \sin(\alpha/2) \cdot \cos(\alpha/2)} \quad [24]$$

and finally

$$a = \frac{\tan(\alpha/2)}{\alpha} \quad [25]$$

Equation 25 is illustrated in Fig. 6, and it is clear that the common approximation that $a = 0.5$ is a valid approximation in edge rolling, in contrast to conventional rolling at geometries encompassing low values of R/h_o, where the deformation pattern is more complicated.[15]

3. Experiments

3.1 *Material*

The material used in this study was extruded, artificially aged aluminum (SS 4212-06) and copper that was continuously cast as 25-mm thick plate, cold rolled to 8 and 6 mm. The goal of cold rolling was to achieve a material that had been deformed to such a degree that further strain hardening would not occur during further deformation, and thus would be approximately ideally plastic during edge rolling experiments. The material was machined to 60 mm wide and 300 mm long plate.

The shear yield stress of the materials was evaluated by means of a standard tensile test. The $R_{p0.2}$ values obtained from the tensile tests were recalculated to true stress, and the shear yield stress was evaluated using von Mises yield criterion.

3.2 *Experimental Equipment*

The experiments were carried out in a universal experimental machine at the University of Luleå. The machine was primarily built for straightening research[18] as a nine-roll roller straightening machine, with 100-mm roller diameter and force measurement on each roll. The machine can also be used for rolling research, for single passes, and for continuous rolling in up to four passes, because the roller velocity can be independently controlled by the individual drive of each roller.

In the edge rolling experiments, the first two rollers were used as a roller guide, with grooved rollers to stabilize the bars. Reduction was carried out in the second pair of rolls. The test equipment is shown in Fig. 7, with the rollers set as in the experiments.

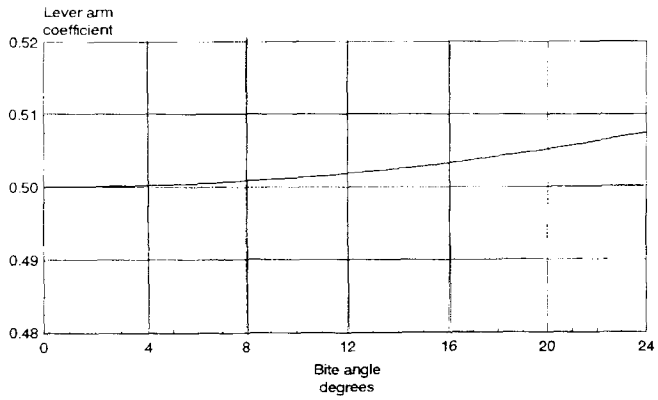

Fig. 6 Lever arm coefficient for edge rolling.

3.3 *Experimental Procedure*

The width and thickness of the bars were measured, and the bars were rolled to different reductions. Roll force was measured during rolling, and the width of the bars was measured after rolling.

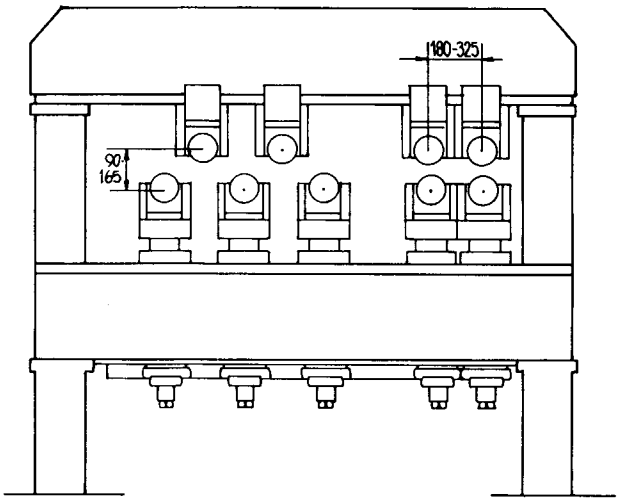

Fig. 7 Universal research machine used for edge rolling trials.

Specimens were cut from the rolled bars, and the shape of the dogbones was measured on a light optical microscope (LOM) micrograph using a magnification of 10×.

The bulk hardness (HV1) and the hardness profiles of the dogbones were taken on the aluminum specimens to evaluate strain distribution over the dogbone.

4. Results

4.1 *Shear Yield Stress*

The shear yield stresses of the test materials are shown in Table 1.

4.2 *Roll Force*

Measured and calculated roll forces are summarized in Table 2.

In Fig. 8, the relationship of $F_{calculated}/F_{measured}$ is illustrated as a function of bite angle. It is clear that the agreement is better in the rolling of aluminum than in the rolling of copper, probably due to the shear yield stress evaluation.

4.3 *Deformation Pattern*

A comparison of the theoretical and measured shape of the dogbone is shown in Fig. 9. The agreement is fairly good. Figure 10 shows the strain distribution over the dogbone of the alu-

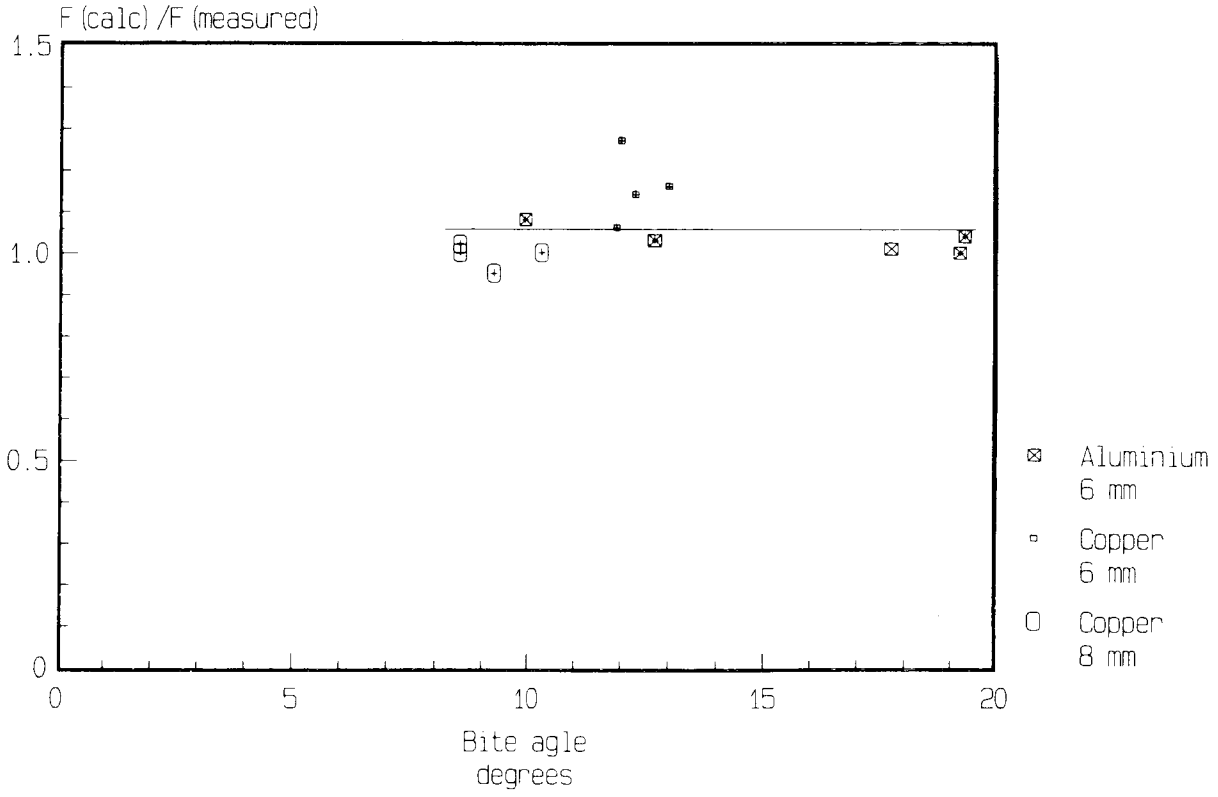

Fig. 8 Agreement between measured and calculated roll force.

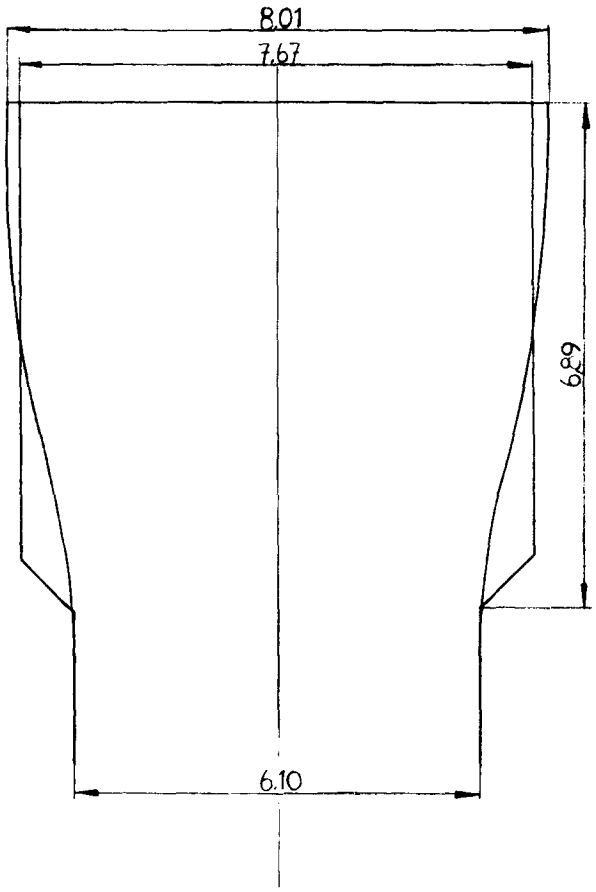

Fig. 9 Theoretical and measured shape of dogbone.

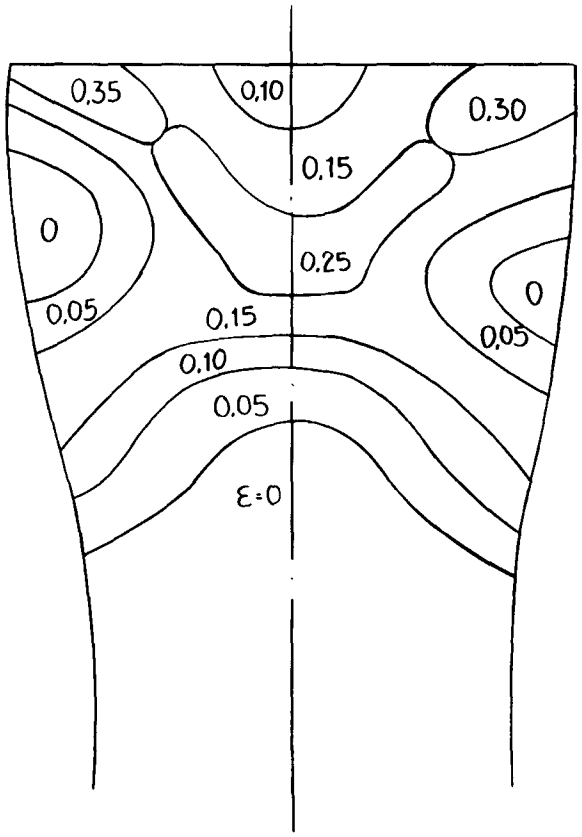

Fig. 10 Strain distribution map of dogbone.

Table 1 Shear yield stress of test materials

Material	Thickness, mm	Shear yield stress, MPa
Copper	8	180.9
Copper	6	217.2
Aluminum	6	169.7

Table 2 Measured and calculated roll force

Material	h_o, mm	$2w_1$, mm	$F_{measured}$, N	$F_{calculated}$, N
Copper	8.55	58.90	23,316	23,395
	8.60	58.90	23,036	23,529
	8.40	58.70	26,407	25,087
	8.40	58.40	27,840	27,862
Copper	6.19	57.85	27,390	29,126
	6.25	57.80	23,316	29,644
	6.26	57.70	26,688	30,470
	6.20	57.45	27,783	32,123
Aluminum	5.95	58.50	16,686	18,060
	6.05	57.55	23,259	23,923
	6.10	55.25	34,636	35,076

minum test piece, rolled to a width equal to 55.25 mm, which was calculated by means of the hardness distribution, the relationship between hardness and yield stress, and the stress-strain curve obtained from the tensile test.

5. Discussion

The agreement between measured and calculated roll forces are very good, at least as far as the aluminum test pieces are considered. The copper tests do not exhibit as good agreement, but must be considered satisfying. From the measurement of strain distribution and from the shape of the dogbones, it is clear that the proposed deformation zone is reasonable. However, it must be remembered that the upper bound method includes some important approximations. First, the shear lines are approximations of the shear zones in the actual deformation mechanisms. Second, the rigid ideally plastic material is an approximation. Real materials are elastic-plastic and do strain harden, and the measurement of strain distribution from hardness distribution would not be possible for an ideally plastic

material. However, strain hardening materials have the ability to change the shape of the deformation zone. The shear zones move into the nondeformed material on the border of the deformation zone, because the movement of the shear bands into the softer nondeformed material reduces the work necessary for deformation.

With the aim to achieve an approximately ideally plastic material, the copper plate was cold rolled before preparation of the specimens. Tensile testing of such heavy cold rolled material is difficult to carry out, because the yield stress is almost equal to the ultimate tensile stress. Thus, the k-values evaluated for copper are much more uncertain than the k-values for the aluminum, which was extruded and aged. This was also the reason for not conducting trials to evaluate the deformation pattern of the copper specimens.

With the good agreement between theory and the experimental results, in combination with the previously reported industrial trials of torque evaluation for edge rolling, the theory is developed to a stage where it can be implemented in a process control system for edge rolling in strip and plate mills and for roll pass design purposes.

Acknowledgment

This research was initiated and financed by Milltek Innovation. Special thanks are due to those persons who made the evaluation of roll force possible—To Professor John A. Schey, University of Waterloo, Ontario, Canada, for providing the idea to use heavily strain-hardened copper and aluminum as approximately ideally plastic materials; To Rolling Mill Supervisor Harald Johnson and Maintenance Supervisor Olle Högberg, Fundia Steel AB, Forsbacka, Sweden, for careful preparation of the test material; To Professor Claes Magnusson, University of Luleå, Sweden, for disposal of the universal test equipment and to B.Sc. Tore Silver, University of Luleå, for valuable assistance in the experimental procedure.

References

1. V.B. Ginzburg, N. Kaplan, F. Bakhtar, and C.J. Tabone, Width Control in Hot Strip Mills, *Iron Steel Eng.*, June, 1991, p 25-39
2. P. Kehl, U. Eggers, J. Ehl, A. Haasler, and W. van Rhee, Erzeugung Schwerer Profile aus Längsgeteiltem Brammenstahlguss bei der Stahlwerke Peine-Salzgitter AG, *Stahl Eisen*, Vol 111 (No. 5), 1991, p 93-99
3. J.-O. Perä, R. Pietola, and U. Sjögren, Optimal Width Reductions in Hot-Strip Mills, *Trans. Iron Steel Inst. Jpn.*, Vol 26, 1986, p 206-211
4. J.G. Beese, Some Problem Areas in the Rolling of Hot Steel Slabs, *Iron Steel Eng.*, Aug, 1980, p 49-52
5. M. Okado, T. Ariizumi, Y. Noma, and Y. Yamazaki, "On the Behavior of Edge Rolling in Hot Strip Mills," Proc. Int. Conf. Steel Rolling, Vol 1, Tokyo, 1980, p 275-286
6. G.J. Heesen, F. Hollander, R.L. Huisman, S. Seijmonsbergen, Large Width Reductions—Physics and Operational Results, *Proc. Conf.* Achieving a Hot Link, London, 1984, p 6.1-6.12
7. S.-E. Lundberg and A. Holmberg, Reduction of Slab Stock by Application of Natural Spread in the Hot Rolling of Plate, *Steel Res.*, No. 7, 1990, p 318-324
8. T. Hope, J.C. Dobson, and K.T. Lawson, "Hi-Spread—A New Hot Rolling Process which Can Effect Major Changes of Slab Width," Proc. Conf. 4th Int. Steel Rolling Conference, Deauville, 1987, p 13.1-13.5
9. O. Pawelski and V. Piber, Möglichkeiten und Grenzen der Umformung in Breitenrichtung beim Warm-Flachwalzen, *Stahl Eisen*, Vol 100 (No. 17), 1980, p 937-949
10. K. Mori, K. Osakada, H. Nikaido, T. Naoi, and Y. Aburatani, "Finite Element Simulation of Non-Steady State Deformation in Rolling of Slab and Plate," Proc. Conf. 4th Int. Steel Rolling Conference, Deauville, 1987, p 6.1-6.8
11. A. Bern, C. David, and J.L. Chenot, "Finite Element Simulation of Spread in Hot Rolling of Thick Slabs," Proc. Conf. 4th Int. Steel Rolling Conference, Deauville, 1987, p 11.1-11.4
12. C. David, C. Bertrand, and J.L. Chenot, "A Transient Three Dimensional Finite Element Analysis of Hot Rolling of Thick Slabs," Proc. NUMIFORM '86 Conf., Gothenburg, 1986, p 219-224
13. M.M. Saf'yan and A.I. Molchanov, Deformation State when Rolling in Stands with Vertical Rolls of Continuous Wide-Strip Mills, *Steel in the USSR*, Sept, 1978, p 517-519
14. S.-E. Lundberg, An Approximate Theory for Calculation of Roll Torque during Edge Rolling of Steel Slabs, *Steel Res.*, No. 7, 1986, p 325-330
15. K. Klarin, J.-P. Mouton, and S.-E. Lundberg, Application of Computerized Slip Line Field Analysis for the Calculation of Lever Arm Coefficient in Hot Rolling Mills, *J. Mater. Proc. Technol.*, Vol 36, 1993, p 427-446
16. Z. Wusatowski, *Fundamentals of Rolling*, Pergamon Press, London, 1969, p 158-195
17. B. Kastner and P. Kastner, Ein Kritischer Beitrag zu der Berechnungsweise des Walzmomentes, *Arch. Eisenhüttenwesen*, Vol 52 (No. 4), 1981, p 147-151
18. I. Sarady, "Riktning av Fartygsprofiler i Rullriktverk (Straightening of Ship Building Angles in a Roller Straightening Machine)," University of Luleå, 1975, p 10-27 (in Swedish)